

Infrared multiphoton ionization of superhot C₆₀: Experiment and model calculations

Anatoly Bekkerman and Eli Kolodney

Department of Chemistry, Technion-Israel Institute of Technology, Haifa 32000, Israel

Gert von Helden^{a)}

Fritz-Haber-Institut der Max-Planck-Gesellschaft, Faradayweg 4-6, D-14195 Berlin, Germany

Boris Sartakov

Fritz-Haber-Institut der Max-Planck-Gesellschaft, Faradayweg 4-6, D-14195 Berlin, Germany, and General Physics Institute, Russian Academy of Sciences, Vavilov Street. 38, 119991, Moscow, Russia

Deniz van Heijnsbergen

FOM Institute for Plasmaphysics, Edisonbaan 14, NL-3439 MN Nieuwegein, The Netherlands

Gerard Meijer

Fritz-Haber-Institut der Max-Planck-Gesellschaft, Faradayweg 4-6, D-14195 Berlin, Germany

(Received 26 January 2006; accepted 15 March 2006; published online 10 May 2006)

We address, both experimentally and theoretically, the issue of infrared (IR) resonance enhanced multiphoton ionization (IR-REMPI) and thermally induced redshifts of IR absorption lines in a very large and highly vibrationally excited molecular system. Isolated superhot C₆₀ molecules with well defined and variable average vibrational energy in the range of 9–19 eV, effusing out of a constant flux thermal source, are excited and ionized after the absorption of multiple (500–800) infrared photons in the 450–1800 cm⁻¹ spectral energy range. Recording the mass-selected ion signal as a function of IR wavelength gives well resolved IR-REMPI spectra, with zero off-resonance background signal. An enhancement of the ion signal of about a factor of 10 is observed when the temperature is increased from 1200 to 1800 K under otherwise identical conditions. A pronounced temperature dependent redshift of some of the IR absorption lines is observed. The observations are found to be in good agreement with a model which is based on the sequential absorption of single photons, always followed by instantaneous vibrational energy redistribution. The mass spectra (C₆₀⁺ fragmentation pattern) are found to be strongly excitation wavelength dependent. Extensive fragmentation down to C₃₂⁺ is observed following the absorption of 1350–1400 cm⁻¹ as well as 1500–1530 cm⁻¹ photons while negligible fragmentation is observed when exciting around 520 cm⁻¹. © 2006 American Institute of Physics. [DOI: 10.1063/1.2193520]

I. INTRODUCTION

Over the last decade C₆₀ has become a valuable model system for studying the behavior of a large and tightly bound molecular system when it is highly excited.¹ The excitation is usually either induced through collisions or via the absorption of photons. The various collisional excitation schemes include C₆₀–buffer gas collisions,^{2,3} C₆₀–surface collisions^{4,5} and electron impact excitation.⁶ Those are all impulsive events that occur on the subpicosecond time scale. The optical excitation is usually induced via UV/visible (VIS) multiphoton absorption where the time scale for the energy deposition is dictated by the laser pulse duration and extends from the femtosecond⁷ to the nanosecond^{8–10} range. Under some experimental conditions, the delayed emission of electrons after electronic excitation using UV/VIS lasers can be observed.^{11,12} Based on internal vibrational energy redistribution (IVR) arguments, it is usually assumed that, on (mass spectrometric) time scales longer than 1 μs, the final distribution of the internal energy within a single C₆₀ mol-

ecule is statistical and the delayed electron emission is thus interpreted in terms of thermionic electron emission. However, the initial excitation step is either not statistical (e.g., any mode of impact excitation on the subpicosecond time scale leading to strongly localized deformations or bond rupture) or is accessing first the electronic subsystem (as in UV/VIS multiphoton absorption). Therefore, processes taking place during the initial energy deposition stage or immediately afterwards are not well defined and the average value of the final (microcanonical) vibrational energy distribution is not known. As a result, the exact nature (both dynamics and energetics) of several fundamental processes in highly vibrational excited fullerenes is still not well understood.

Recently, the excitation and ionization of fullerenes (C₆₀, C₇₀, C₈₄) following the extreme multiphoton absorption of IR radiation from a free electron laser for infrared experiments (FELIX) was demonstrated.^{13–18} The resonant absorption of an estimated 30–50 eV total energy per single C₆₀ molecule, directly deposited into vibrational modes, results eventually in quasithermal conditions leading to delayed electron emission. The unique combination of resonant mo-

^{a)}Electronic mail: helden@fhi-berlin.mpg.de

molecular absorption of hundreds of IR photons and thermionic emission enables one to measure the so-called infrared resonance enhanced multiphoton ionization (IR-REMPI) spectrum.¹³ This spectrum appears to be quite similar to the linear IR absorption spectrum of C_{60} as far as the spectral location of IR active modes is concerned. However, the relative intensities of the absorption lines can be different, mainly due to the dynamics of the absorption of very many photons. The excitation by FELIX photons is distinct from all other excitation schemes since the energy is being deposited rather slowly and gently (during a few microseconds) directly into vibrations, and the final internal energy distribution of an ensemble of C_{60} molecules can be similar in shape to a thermal one, although much narrower.^{17,18} However, as with all other excitation modes the final energy deposited in the C_{60} molecule (the average vibrational energy in this case) is unknown and can only be roughly estimated. When the excitation is performed with comparatively low IR fluences, signs of nonstatistical behavior in the electron emission kinetics could be observed.¹⁴ This is interpreted in terms of nonequilibration of energy within the molecule, possibly caused by bottlenecks in phase space.

Via a different experimental approach, based on the method of generating an effusive molecular beam of superhot species using a two stage capillary nozzle assembly, it has been demonstrated that a stable flux of thermally excited C_{60} can be produced with average internal vibrational energy \bar{E}_{th} in the range of 10–20 eV, corresponding to nozzle temperatures T_N of 1000–2000 K.^{19,20} The calibrated and highly reproducible performance of this source has been used to advantage in several recent studies addressing the quasithermal behavior of vibrationally excited C_{60} molecules.^{19–24} While the superhot thermal source method can not access the very high internal excitation range above 20 eV, it is presently the only method that can provide a controlled and well defined deposition of essentially pure vibrational thermal energy into C_{60} molecules with a well defined canonical distribution. The combination of the thermally tunable superhot C_{60} source with the ability of FELIX to resonantly heat thus provides a unique opportunity to study the behavior of an ensemble of extremely vibrationally excited C_{60} molecules ($\bar{E}_{th}=50$ –100 eV) in a well controlled way. The coupled superhot source/FELIX approach is especially suited for studying the thermal energy dependence of a given process over the $\delta\bar{E}_{th}=10$ eV range on which some \bar{E}_{FELIX} internal excitation is superimposed, by keeping the FELIX intensity fixed and scanning the nozzle source temperature. In this paper we have addressed, both experimentally and theoretically, the issue of IR multiphoton ionization and dissociation, and thermally induced redshifts of IR absorption lines, in extremely vibrationally excited C_{60} molecule. We will describe IR-REMPI experiments based on the excitation and ionization of superhot C_{60} molecules ($\bar{E}_{th}=9$ –19 eV) via IR radiation from FELIX over the 450–1800 cm^{-1} frequency range.

The measurements are also highly relevant with respect to fundamental spectroscopic issues related to the behavior of superhot large molecules. It is for example not clear if a large polyatomic molecule at a temperature of almost

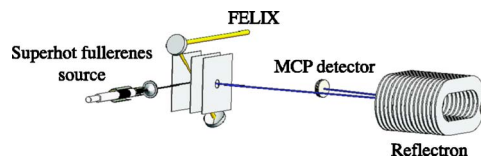


FIG. 1. Scheme of the experimental setup. C_{60} is evaporated and heated to high temperatures before it forms an effusive beam. The molecules are then overlapped with FELIX and ions are detected in a time of flight (TOF) mass spectrometer.

2000 K still has a well defined spectrum or whether the high density of states causes vibrational coupling and broadening, so that the molecule effectively absorbs at any wavelength. This point is important, as it is frequently stated that only the first few IR photons in a molecule are absorbed resonantly and subsequent excitation can be performed at any wavelength. Here we will show that, at least for C_{60} , this is not the case and even superhot C_{60} does not absorb where, for example, a CO_2 laser emits, near 10 μm .¹⁰

II. EXPERIMENT

The experimental setup is schematically presented in Fig. 1. It consists of the Technion two stage effusive source for superhot C_{60} ^{19–24} which is interfaced to the cluster molecular beam machine¹⁸ at the research institute Rijnhuizen of the Stichting voor Fundamenteel Onderzoek der Materie (FOM). The beam of superhot C_{60} can then be irradiated by the tunable IR radiation, emitted from FELIX.¹⁸ FELIX is a source of intense, tunable IR radiation. The light output comes in macropulses of about 5 μs duration, containing 0.3–5 ps long micropulses at a spacing of 1 ns. The tuning range spans the 40–4000 cm^{-1} range, although only the 500–2000 cm^{-1} region is used in the present experiments. The energy in a macropulse can exceed 100 mJ and the maximum macropulse repetition rate is 10 Hz. The bandwidth is transform limited and user adjustable and can range from 0.5% full width at half maximum (FWHM) to several percent of the central frequency. As has been reported earlier,¹³ C_{60} molecules can resonantly absorb several hundred photons and then ionize due to the thermal emission of an electron. The resulting ionic products can be detected after passing through a reflectron time of flight mass spectrometer. FELIX is then scanned, and mass spectra are recorded as a function of FELIX wavelength. Infrared spectra are then generated by integrating the ion signal over the mass peaks of interest and plotting that quantity versus FELIX wavelength. The mass spectra shown in the figures in this paper are generated by adding mass spectra at different FELIX wavelengths over an absorption envelope.

The main technical challenge in this experiment was the coupling of the Technion superhot C_{60} source with the FELIX—molecular beam machine. The two stage source is mounted on an adjustable base plate and was built, conditioned, and calibrated at the Technion before installation and testing at FOM-Rijnhuizen. Two source assemblies were interchanged during the experiments and the results were practically identical. Details of the superhot C_{60} source and its temperature measurements are given elsewhere.^{19,20} Briefly, it is a two stage oven where C_{60} vapor that is generated in the

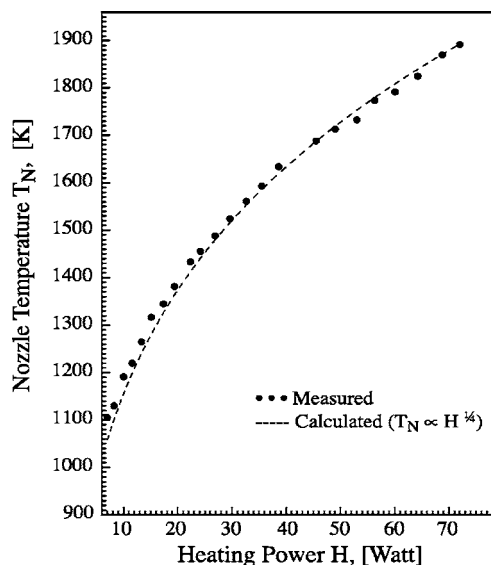


FIG. 2. Temperature as a function of heating power for the superhot C₆₀ oven.

first oven stage flows through a high temperature (up to 2100 K) capillary nozzle stage after which it forms an effusive beam with a nearly constant ($\pm 5\%$) flux of superhot C₆₀ molecules. The beam temperature, as measured by time of flight (TOF) thermometry, was found to be in good agreement with micro-optical pyrometry of the nozzle aperture.¹⁹ The whole assembly is constructed as a vacuum tight all ceramic (alumina) unit. The capillary nozzle stage is mounted at the end of a long ceramic tubing and is fully thermally decoupled from the first stage, thus assuring a nearly constant flux. The whole source assembly including its multiple radiation shields (tantalum, ceramics) constitutes a nearly perfect blackbody radiator. Figure 2 shows the final temperature of the nozzle aperture (as measured by micro-optical pyrometry) as a function of the heating power H along with a calculated $H = A_{\text{eff}} \epsilon \sigma T_N^4$ curve where σ is the Stefan-Boltzman constant, ϵ is the emissivity constant (taken as one), and where the effective (fitted) area is $A_{\text{eff}} = 0.995 \text{ cm}^2$.

The agreement with a T^4 law is very good over the 1200–1900 K range thus demonstrating that the relative contribution due to conductance heat losses is negligible. The power-temperature calibration curve served for highly reproducible and reliable thermometry of the nozzle aperture and of the C₆₀ beam with an estimated accuracy of ± 20 K. Minor effects of radiative energy losses during the flight time of hot C₆₀, from the moment it exits the nozzle until FELIX excitation, will be discussed later on.

III. RESULTS

The IR-REMPI spectrum of 1790 K hot C₆₀ is obtained by recording the mass-selected C₆₀⁺ yield as a function of the FELIX frequency and is shown in Fig. 3. Clearly five peaks can be observed. On the base line, no ions are detected and the noise there is given by detector noise. The spectrum is similar to the “low temperature” (875 K) IR-REMPI spectrum observed previously,¹³ and the five lines can be as-

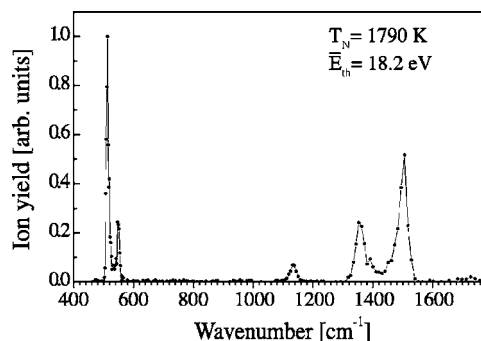


FIG. 3. IR-REMPI spectrum of C₆₀ at a source temperature of 1790 K.

signed to the four IR allowed F_{1u} fundamental modes of icosahedral C₆₀ and an IR allowed combination band. We will label the bands from low to high energy as $F_{1u}(1)$, $F_{1u}(2)$, $F_{1u}(3)$, $F_{1u}(4)$, and I_{comb} , respectively.

The 1790 K hot C₆₀ molecules have an average internal energy of $\bar{E}_{\text{th}} = 18.2 \text{ eV}$. This is much more than the ionization energy of C₆₀ (7.61 eV), however, still much less than the 40–50 eV of internal energy required for C₆₀ to ionize on the microsecond time scale (*vide infra*). The latter internal energies can be obtained by the repeated resonant absorption of single IR photons followed by IVR. A detailed model will be presented later in this contribution. Due to anharmonicities and cross anharmonicities, the high internal energy of C₆₀ will give rise to redshifts of the vibrational modes. In addition, the coupling of the IR active modes to the increased density of other vibrational and electronic states will cause line broadening. The density of vibrational states at an internal energy of 18 eV is, for example, $> 10^{100}$ states/cm⁻¹. It was thus *a priori* not clear whether an IR-REMPI spectrum with resolved lines was to be expected and how it would relate to the IR-REMPI spectrum obtained at lower temperature. As already mentioned, the spectrum exhibits the same absorption lines observed in the previously reported low temperature (875 K) gas phase IR-REMPI spectrum of C₆₀.¹³ Relative peak intensities are generally similar but not identical. For example, the relative peak intensity of the $F_{1u}(3)$ mode at 1136 cm⁻¹ is significantly smaller while the $F_{1u}(2)$ peak at 550 cm⁻¹ [the smaller one to the right of the 515 cm⁻¹ $F_{1u}(1)$ peak] is significantly more intense in the 1790 K spectrum, compared to the 875 K spectrum. Also, the positions of all the high temperature IR-REMPI lines are redshifted with respect to their positions in the previously

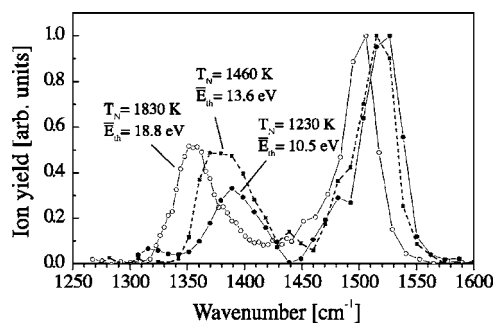


FIG. 4. IR-REMPI spectra of C₆₀ in the range between 1250 and 1600 cm⁻¹ for three different temperatures of the C₆₀ source.

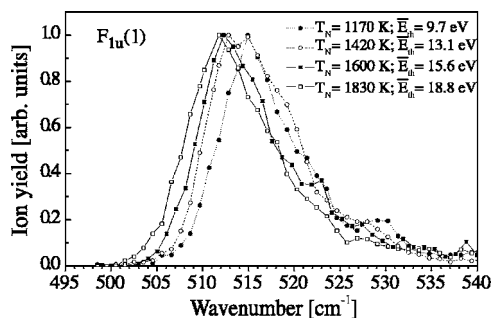


FIG. 5. IR-REMPI spectra of C_{60} in the range between 495 and 540 cm^{-1} for four different temperatures of the C_{60} source.

reported low temperature spectrum¹³ which, by themselves, are redshifted with respect to the emission lines of hot gas phase C_{60} .²⁵

The temperature dependence of the IR-REMPI lines between 1250 and 1600 cm^{-1} is shown in Fig. 4 and that of the $F_{1u}(1)$ mode near 515 cm^{-1} is shown in Fig. 5. In both figures, the spectra are normalized to the largest peak. Clearly all peaks shift to the red as the temperature is increased. The most prominent redshift is observed for the $F_{1u}(4)$ IR-REMPI line whose peak value shifts from 1390 cm^{-1} at $\bar{E}_{th} = 10.5$ eV to 1355 cm^{-1} at $\bar{E}_{th} = 18.8$ eV. Such a large shift is qualitatively expected for this mode, as it has the largest anharmonicity coefficient of all the four IR active modes of icosahedral C_{60} .¹⁷ The redshift of the low frequency $F_{1u}(1)$ IR-REMPI line is with about 4 cm^{-1} , when going from 1170 to 1830 K nozzle temperature, much smaller. Another observation is that the small shoulder at 1480 cm^{-1} (also observed at the low temperature FELIX spectrum,¹³ possibly resulting from a weak combination band) gradually disappears with increasing temperature. The width of the peaks is nearly independent of the temperature with the exception of some narrowing that is observed in the $F_{1u}(4)$ when going from $T_N = 1460$ K to $T_N = 1830$ K (see Fig. 4). Note the pronounced asymmetry in the line shape of the $F_{1u}(1)$ mode in Fig. 5; at all temperatures, the peak is observed to have a tail to the high photon energies. This asymmetric line shape has been discussed before^{13,17} and can be explained by the dynamics of the photon absorption process.

As mentioned already, the intensities of the spectra shown in Figs. 4 and 5 are scaled. The peak intensities are

observed to depend strongly on the FELIX parameters such as power and bandwidth as well as on the source temperature. It is observed that increasing the source temperature from around 1200 K to around 1800 K results in a signal increase of about a factor of ten. The source produces a nearly constant flux of C_{60} . The velocity of the molecules scales with $\sqrt{T_N}$. The interaction time of the molecules with FELIX is not so much determined by the FELIX pulse length but mainly by the time it takes for the molecules to traverse the IR-irradiated volume. The hotter molecules thus have a shorter interaction time with FELIX. However, it is observed that this is more than compensated for by the increase in initial internal energy.

A comparison between spectral peak positions of the IR-REMPI lines under the different experimental conditions is presented in Table I. Given are the positions of superhot C_{60} IR-REMPI lines at 1230 and 1830 K (this experiment) and the positions of the low temperature C_{60} IR-REMPI lines.¹³ For comparison, the positions of the IR-emission lines of hot gas phase C_{60} ,²⁵ the IR absorption lines of solid C_{60} at room temperature²⁶ as well as the line positions obtained from theory²⁷ are also given.

When inducing thermionic emission using UV or visible lasers, a large amount of fragmentation is usually observed.¹² Contrary, using IR light, only a small amount of fragmentation is observed. In Fig. 6, mass spectra are shown that are obtained by adding up mass spectra over the corresponding IR-REMPI peak. The nozzle temperature is 1830 K in all these cases. In the upper panel, the mass spectrum obtained after excitation on the $F_{1u}(1)$ mode is shown. Only a small amount of fragmentation leading to C_{58}^+ and C_{56}^+ is observed. When exciting at 1355 and 1500 cm^{-1} , a substantial amount of fragmentation is observed, as shown in the lower two mass spectra. In both spectra, the lowest mass observed is C_{32}^+ . Fullerenes are known to fragment via sequential C_2 loss. For fullerenes in the C_{40} to C_{90} size range, the dissociation energy for C_2 loss is usually assumed to be between 8 and 11 eV.²⁸ The observation of fragments as small as C_{32}^+ therefore implies that on the order of 14×9 eV = 126 eV of additional energy have to be deposited via IR absorption into the system! Even if most of the fragmentation below C_{40}^+ is dominated by a cleavage mechanism (leading to C_m^0 , $m = 4, 6, \dots$ emission),² this rough estimation still holds. The

TABLE I. Positions of C_{60} IR-REMPI lines at different temperatures. Also shown are IR emission and IR linear absorption line positions as well as line positions obtained from theory.

Experiment	IR-REMPI ^a 875 K	IR-REMPI ^b 1230 K	IR-REMPI ^b 1830 K	Emission ^c 950 K	Absorption ^d 300 K	Theory ^e 0 K
$F_{1u}(1)$	518	515	511	528	526	528
$F_{1u}(2)$	557	...	550	570	576	577
$F_{1u}(3)$	1145	...	1136	1171	1183	1189
$F_{1u}(4)$	1397	1391	1355	1411	1429	1431
I_{comb}	1525	1517	1503	1539	1538	...

^aSee Ref. 11.

^bThis work.

^cSee Ref. 25.

^dSee Ref. 26.

^eSee Ref. 27.

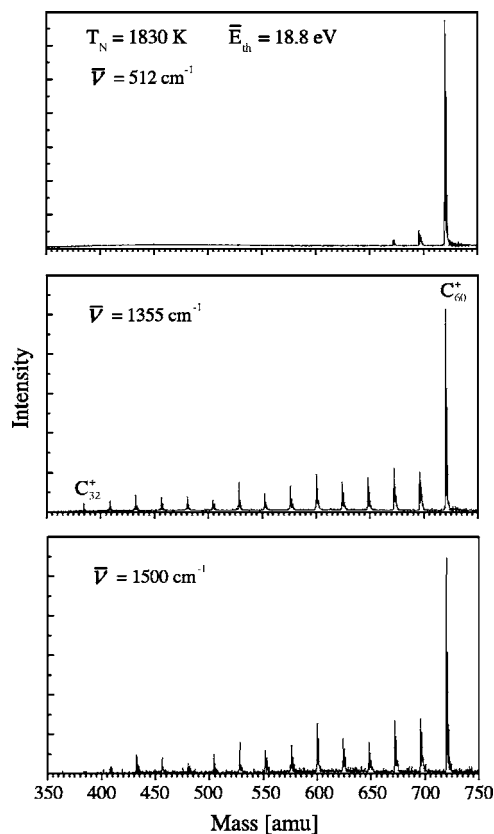


FIG. 6. Mass spectra obtained after exciting superhot C₆₀ on different modes.

relative fragment ion intensities in the mass spectra are observed to be nonmonotonous and the relative high intensity of, for example, C₅₀⁺ might reflect its enhanced stability. It is also important and interesting to note that the relative amount of fragmentation is only weakly dependent on laser power. For example, increasing the IR-laser power when exciting on the $F_{1u}(1)$ mode to its maximum value does not substantially increase the amount of fragmentation while lowering the IR-laser power when exciting on the other modes still gives a similar relative amount of fragmentation, until the total signal disappears.

IV. THEORETICAL MODELING

A. Fullerene structures and linear IR spectra

To reach a quantitative understanding of the observed IR-REMPI spectra of C₆₀ and to explain the wavelength dependent fragmentation pattern of C₆₀, the vibrational frequencies and the (linear) IR absorption spectrum for C₆₀ as well as for two C₅₈ isomers in their neutral as well as in their singly positively charged form have been calculated using density functional methods. This is needed to investigate the possibility of resonant multiple photon excitation of the C₆₀⁺ ion and/or of neutral or charged C₅₈ fragments during the IR excitation pulse. The calculations are performed with the Becke3LYP functional and the 6-31G(d) basis set using the program GAUSSIAN03. The geometries of the structures are fully optimized and analytical second derivatives are calculated. All calculated structures represent minima on the po-

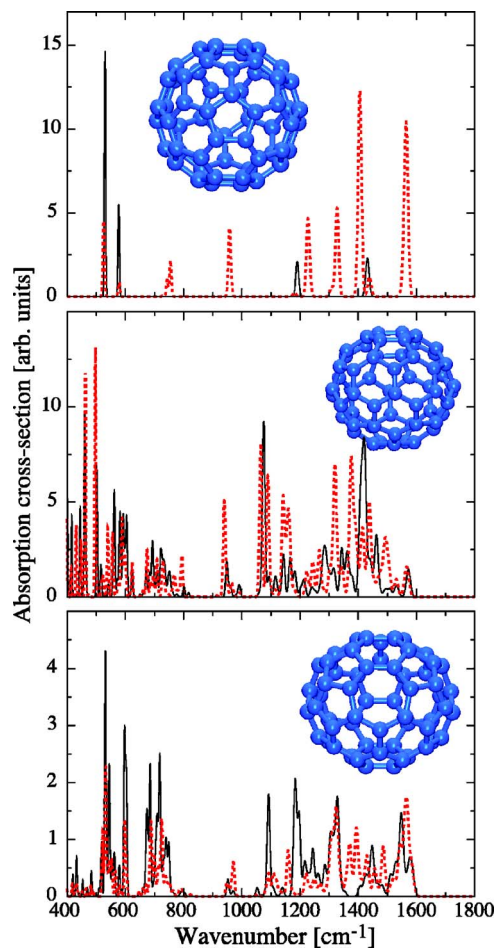


FIG. 7. Calculated linear IR absorption spectra of C₆₀ (top), C₅₈ (five and six membered rings only, center), and C₅₈ (one 7 membered ring, bottom). The spectra for neutral species are shown as solid lines and for the ionic molecules as dashed lines.

tential energy surface. For neutral C₆₀, the IR spectrum is calculated with the molecule having I_h symmetry. The C₆₀⁺ is known to undergo Jahn-Teller distortion and the calculation is performed in D_{5d} symmetry. Two different C₅₈ isomers have been considered and both of them, including their ions, have C_s symmetry. Both isomers have been considered before,^{29–31} and the relative stabilities and ionization energies obtained from the calculations presented here are identical with those obtained by others.^{30,31}

The calculated IR spectra are shown in Fig. 7. They are obtained by convoluting the calculated stick spectrum with a Gaussian having a FWHM of 1% of the corresponding central frequency. The spectra for the neutral species are shown as solid lines and the spectra of the ions are shown as dashed lines. The spectra shown in the upper panel are for C₆₀ and C₆₀⁺ while the lower two panels show spectra for the two C₅₈ and C₅₈⁺ isomers. The neutral C₅₈ isomer, shown in the middle panel, contains three pairs of two adjacent pentagons and is calculated to be 0.1 eV lower in energy, compared to the isomer shown in the lower part of the figure, which contains one heptagon and two chains of three adjacent pentagons.

For neutral C₆₀, four IR active modes are calculated. The calculated modes for C₆₀ are identical to those obtained by

others²⁷ and are in good agreement with experimental values.²⁶ Upon ionization, the symmetry of the molecule is reduced and many more modes become IR active. In addition, the intensity pattern changes. Most notably, the strongest mode in the neutral near 530 cm⁻¹ loses a factor of about 3 in intensity when the molecules are ionized. In contrast to that, in the higher frequency range near 1500 cm⁻¹, new modes become IR active and the strongest of them are more than a factor of 4 more intense than the strongest modes for the neutral in that range. Therefore, when C₆₀ ionizes during the IR pulse, the C₆₀⁺ ion can resonantly absorb many more photons, in particular, when originally excited on the *F*_{1u}(4) or on the combination band *I*_{comb} of C₆₀.

In the C₅₈ isomers, the symmetry is largely reduced compared to C₆₀. As a consequence, many more modes are IR active. It is also noticeable that the IR spectrum of the low energy C₅₈ isomer shown in the middle in Fig. 7 has generally more IR intensity, than the C₅₈ isomer shown in the lower part of the figure. An important consequence of the high density of IR active modes is that when C₆₀ or C₆₀⁺ would fragment within the time that the IR laser is on (5 μs), the resulting C₅₈ or C₅₈⁺ molecules could be resonant with the IR field and absorb additional photons. In such a scenario, fragments could thus be efficiently heated with the result of extensive fragmentation. This point will be further discussed later.

B. Excitation mechanism

As C₆₀ is a large molecule, many vibrational modes are present and the density of vibrational states as well as its heat capacity can be very high. For example, when C₆₀ effuses from the oven at 800 K, its mean internal energy is 39 000 cm⁻¹ and the density of states at this energy is 10⁴⁸ states/cm⁻¹. The density of vibrational states rapidly climbs to much larger values at higher energies, and the coupling between these many states due to vibrational anharmonicities results in very fast internal vibrational energy redistribution (IVR). It is therefore safe to assume that the IVR process, the rate of which is determined by the intermode anharmonicity of the molecule, is much faster than the rate of photon absorption. Indeed, the anharmonicity constants of molecules are typically of the order of 1–10 cm⁻¹, thus one can expect the characteristic time of the IVR process to be on the subpicosecond time scale. The time scale for the rate of photon absorption in the 5 μs duration pulse is much longer. The vibrational energy is then at any time statistically distributed over the vibrational degrees of freedom and the excitation process can be described using a statistical approach. It is also expected that, due to the high density of states and the coupling between them, coherent excitation effects, such as rapid adiabatic passage, are not important in the experiments described here. The rate of laser induced transitions *i* → *j* (one photon absorption or emission) between the levels in the dense vibrational energy spectrum can be expressed by using Fermi's golden rule as

$$w_{i,j} = \frac{2\pi}{\hbar} |V_{i,j}|^2 \rho(E_j) \delta(E_j - E_i \mp \hbar\omega), \quad (1)$$

where *V*_{*i,j*} is the matrix element of the molecule-laser field interaction *V* and $\rho(E_j)$ is the energy density of the final states in the vicinity of *E_j*. The delta function $\delta(E_j - E_i \mp \hbar\omega)$ assures the realization of the energy conservation law in the process of one photon absorption/emission and shows that the resonant laser induced absorption/emission processes couples the levels within the ladder defined as *E_i* = *E*₀ + *i*ħω, here *E*₀ is the lowest energy level in the ladder and *i* = 0–∞ enumerates the ladder levels.

The dynamics of the population distribution in the ladder of resonant vibrational levels can be described by the kinetic equations

$$dn_i/dt = k_{i+1,i}n_{i+1} + k_{i-1,i}n_{i-1} - k_{i,i+1}n_i - k_{i,i-1}n_i, \quad (2)$$

where *n_i* is the population of the *i*th level and the rates of laser induced transitions are defined as *k_{i,j}* = (2π/ħ)|*V_{i,j}*|²ρ(*E_j*) in accordance with Fermi's golden rule.

As the interaction between the laser field and the molecule in our case is determined by the dipole interaction *V* = -**E** · **μ**, where **E** is the electric field strength and **μ** is the dipole moment operator of the molecule, we can rewrite the formula for the rate of transitions in the form generally accepted in spectroscopy as

$$k_{i,j} = \frac{I}{\hbar\omega} \sigma_{i,j}, \quad (3)$$

where *I* = |**E**|²/8π*c* is the intensity of the laser radiation and $\sigma_{i,j}$ is the absorption cross section.

The cross sections of up (*i* → *i* + 1) and down (*i* + 1 → *i*) transitions must satisfy the principle of detailed balance,

$$\sigma_{i,i+1}/\sigma_{i+1,i} = \rho(E_{i+1})/\rho(E_i), \quad (4)$$

that is consistent also with Fermi's golden rule.

The dependence of the absorption cross section $\sigma_{i,i+1}(\nu)$ on the laser frequency ν is usually characterized by the rather sharp resonances which can be assigned either to the IR active vibrational modes of the molecule or to the vibrational combination band of the molecule. The width of the resonances is normally much less than the vibrational frequencies of the molecule. The physical reason for this is that the rate of the IVR process, which determines the broadening of the resonances and which is of the order of magnitude of the vibrational anharmonicity, is much lower than the vibrational frequencies. So, in the vicinity of the resonance frequency $\nu^{(m)}$ the absorption cross section can be represented as

$$\sigma_{i,i+1}(\nu) = A_{i,i+1}^{(m)} f^{(m)}(\nu - \nu^{(m)}), \quad (5)$$

where $A_{i,i+1}^{(m)}$ is the integral absorption cross section of the *m*th vibrational band for the transition *i* → *i* + 1 and where $f^{(m)}(\nu - \nu^{(m)})$ is the resonance form factor which is different from zero only in the vicinity of the vibrational mode resonance frequency $\nu^{(m)}$ and which is normalized in a such way that

$$\int_{\nu \sim \nu^{(m)}} f^{(m)}(\nu - \nu^{(m)}) d\nu = 1.$$

There are two strong resonances in the multiphoton spectra which can be assigned to the IR active fundamental vibrational modes of C₆₀. The strongest resonance is near 520 cm⁻¹, and the next strongest one is near 1400 cm⁻¹. The resonance near 1500 cm⁻¹ cannot be assigned to a fundamental IR vibrational mode of the C₆₀ molecule, and it likely corresponds to a combination band. In solid C₆₀, a moderately strong absorption is observed at 1538 cm⁻¹.²⁶ A possible candidate for this mode is the binary combination of the G_u(3) mode and the F_{2g}(3) mode. Theory (see above as well as Ref. 27) predicts this combination band to occur at 751 cm⁻¹+789 cm⁻¹=1540 cm⁻¹.

In the case of IR active fundamental modes the dependence of the integral absorption cross section on the vibrational energy of the molecule is modeled with the following formula:

$$A_{i,i+1}^{(m)} = A_0^{(m)} \cdot (1 + \langle v^{(m)}(E_i) \rangle / g^{(m)}). \quad (6)$$

Here $A_0^{(m)}$ is the integral absorption cross section of the fundamental $v^{(m)}=0 \rightarrow v^{(m)}=1$ transition of the m th mode which can be measured by means of linear spectroscopy or which can be obtained via *ab initio* calculations. The linear dependence on the statistical mean value of vibrational quanta of the m th mode $\langle v^{(m)}(E_i) \rangle$ follows from Fermi's golden rule formula. It is furthermore based on the assumption that, by analogy with the harmonic oscillator, the square of the dipole moment matrix element rises linearly with the vibrational quantum number $v^{(m)}$ of the m th mode, e.g., proportionally to $1 + v^{(m)}/g^{(m)}$, where $g^{(m)}$ is the degeneracy of m th mode. The replacement of $v^{(m)}$ by its statistically averaged value corresponds to the assumption that the IVR process results in a fast statistically averaged redistribution of the vibrational energy between all vibrational modes of the molecule.

In the case of binary combination bands the dependence of the integral absorption cross section on the statistical mean values of vibrational quanta can be very complicated. First, because the dipole moment of the combination vibration is determined by the second derivative of the dipole moment function $(\partial^2 \hat{\mu} / \partial q_m \partial q_k) q_m q_k$ and is a quadratic function of the vibrational coordinates q_m and q_k . As a consequence, the square of the dipole moment matrix element rises nonlinearly with the vibrational quantum numbers. Second, the combination bands can borrow dipole moment strength from the IR active modes by virtue of the anharmonic interaction which is increasing nonlinearly with the increase of vibrational energy.

The integral absorption cross section of the binary combination band near 1500 cm⁻¹ is modeled as

$$A_{i,i+1}^{(c)} = A_0^{(c)} (1 + \langle v^{(m)}(E_i) \rangle / g^{(m)}) (1 + \langle v^{(k)}(E_i) \rangle / g^{(k)}). \quad (7)$$

Here $A_0^{(c)}$ is the integral absorption cross section of the transition $0 \rightarrow \nu_c$ and the factors $(1 + \langle v^{(m)}(E_i) \rangle / g^{(m)})$ are used here to model the nonlinear (quadratic) increase of the integral cross section with the increase of the mean value of the vibrational quanta in the m th vibrational mode.

To calculate the statistically averaged value of vibrational quanta in the m th mode the molecule possessing the

vibrational energy E was treated as a thermodynamical ensemble of harmonic oscillators at an effective temperature T_{eff} , i.e.,

$$E = \sum_m \frac{g^{(m)} \hbar \omega^{(m)}}{\exp(\hbar \omega^{(m)} / k T_{\text{eff}}) - 1}.$$

The statistically averaged number of quanta in the m th mode is determined in this case via

$$\langle v^{(m)}(E) \rangle = \frac{g^{(m)}}{\exp(\hbar \omega^{(m)} / k T_{\text{eff}}) - 1}$$

The resonance shape function $f^{(m)}(\nu - \nu^{(m)})$ is taken as a normalized Lorentzian function,

$$f^{(m)}(\nu - \nu^{(m)}) = \frac{\Gamma^{(m)}}{\pi [(\nu - \nu^{(m)})^2 + (\Gamma^{(m)})^2]}. \quad (8)$$

Here ν_m is used to designate either the vibrational mode frequency or the combination mode frequency. We assumed that both the width of the Lorentzian (FWHM) $\Gamma^{(m)}$ and the deviation of the resonant frequency $\nu^{(m)}$ from its harmonic value $\nu_0^{(m)}$ originate from the anharmonicity of molecule vibrations, which can be considered as a small perturbation of harmonic oscillations. Thus in the first order of perturbation both parameters can be approximated by a linear dependence on the vibrational level energy $E_i = E_0 + i \hbar \omega$,

$$\Gamma^{(m)}(E_i) = b^{(m)} i, \quad \nu^{(m)}(E_i) = \nu_0^{(m)} - a^{(m)} i. \quad (9)$$

The expression for $\sigma_{i,j}(\nu)$ was also convoluted with the spectral profile of the excitation radiation, which was assumed to be a Lorentzian as well.

The 0 K frequency positions of the three modes considered were taken from *ab initio* theory²⁷ and held fixed. The parameters a and b were first estimated from temperature dependent emission studies of gas-phase C₆₀ (Ref. 25) and then fitted to get the best agreement between simulated and experimental ion yield spectra. The integral absorption cross sections of the fundamental vibrational modes were taken from the *ab initio* calculations and held fixed. The integral absorption cross section of the combination band near 1550 cm⁻¹ was fitted.

The rate equations (2) for the energy level population were supplemented with the decay terms accounting for the ionization and the dissociation of excited molecules,

$$\begin{aligned} dn_i/dt = & k_{i+1,i} n_{i+1} + k_{i-1,i} n_{i-1} - k_{i,i+1} n_i - k_{i,i-1} n_i \\ & - (K_D(E_i) + K_I(E_i)) n_i, \end{aligned} \quad (10)$$

where $K_D(E_i)$ and $K_I(E_i)$ are, respectively, the rates of the dissociation and the ionization of C₆₀. In previous experiments, nonstatistical behavior of the ionization rate after IR excitation could be observed.¹⁴ This effect was, however, only significant at laser fluences that are a factor of 3–5 lower than those used in the present experiments. The ionization rate via the channel C₆₀^{*} → C₆₀⁺ + e and the dissociation rate via the channel C₆₀^{*} → C₅₈ + C₂ for a given vibrational energy of C₆₀^{*} were therefore calculated by using the rate parameters presented in Ref. 32. Running the simulation showed that, for the parameter range considered, the dissociation of C₆₀ or C₆₀⁺ did only influence the spectra in the

form of a scaling of the vertical axis. As the experiment does not measure absolute intensities, a fitting of the dissociation parameters is not useful and we therefore arbitrarily set the dissociation rate to zero.

The initial population distribution over the vibrational levels of C_{60} was assumed to be thermal: $dn(E)/dE = \rho(E)\exp(-E/kT)/Z$; here $\rho(E)$ is the density of vibrational states, T is the vibrational temperature taken as equal to the nozzle temperature T_N , and Z is the partition function. In principle, one has to consider also some energy loss due to radiative cooling of the superhot C_{60} during its flight time from the nozzle aperture to the FELIX excitation zone (0.66 ms average value). A simple calculation based on a commonly used expression for the radiative energy loss rate³³ yields about 1 eV energy loss for the highest nozzle temperature of 1830 K (upper limit) and much smaller losses for the lower temperature values. Some details are given in Ref. 34. The time evolution of the (initially canonical) energy distribution due to radiative cooling was considered before.³⁵ The distribution was shown to be gradually shifted but only slightly distorted. Summarizing, these two radiative cooling effects were found to be below the sensitivity of our simple model calculation and will therefore not be taken into account.

The actual geometry of the focused FELIX beam and the effect of the C_{60} in the effusive beam moving through the focus is explicitly taken into account in the calculation. For a set of initial coordinates of the C_{60} molecules $\{x_0, y_0, z_0\}$, we simulated the trajectories $\{x(t) = x_0 + v_x t, y_0, z(t) = z_0 + v_z t\}$ through the FELIX beam with the angle between the velocity vector \mathbf{v} of the molecules and the laser beam direction (here assumed as z direction) being $\Theta = 23^\circ$. In the experiment the effusive molecular beam was rather well collimated by a small aperture. The density distribution over the molecular velocities was taken to be thermal: $p(v) \sim v^2 \exp(-mv^2/2kT)$, with m the mass of the C_{60} molecule and T the translational temperature, taken as equal to the nozzle temperature.

The spatial profile of the laser beam is taken to be Gaussian,

$$I(x, y, z) = \frac{E_{\text{laser}}}{\pi r_x(z) r_y(z) T_{\text{laser}}} \exp\left[-\frac{x^2}{r_x^2(z)} - \frac{y^2}{r_y^2(z)}\right],$$

where E_{laser} is the energy of the laser macropulse, T_{laser} is the duration of the macropulse and $r_x(z)$ and $r_y(z)$ are the radii of the laser beam. The astigmatism of the focusing system was taken into account and the radii of the laser beam were calculated as

$$r_x(z) \approx \sqrt{r_0^2 + [(z + \delta)/(2\pi\nu r_0)]^2},$$

$$r_y(z) \approx \sqrt{r_0^2 + [(z - \delta)/(2\pi\nu r_0)]^2},$$

with r_0 the radius at the focus waist and 2δ the distance between the focus waist in the x and y directions. The parameters r_0 and δ are calculated for a given laser wave number assuming that the incident laser beam is a diffraction limited Gaussian beam, having a radius of about 5 mm and taking into account that focusing is achieved by a

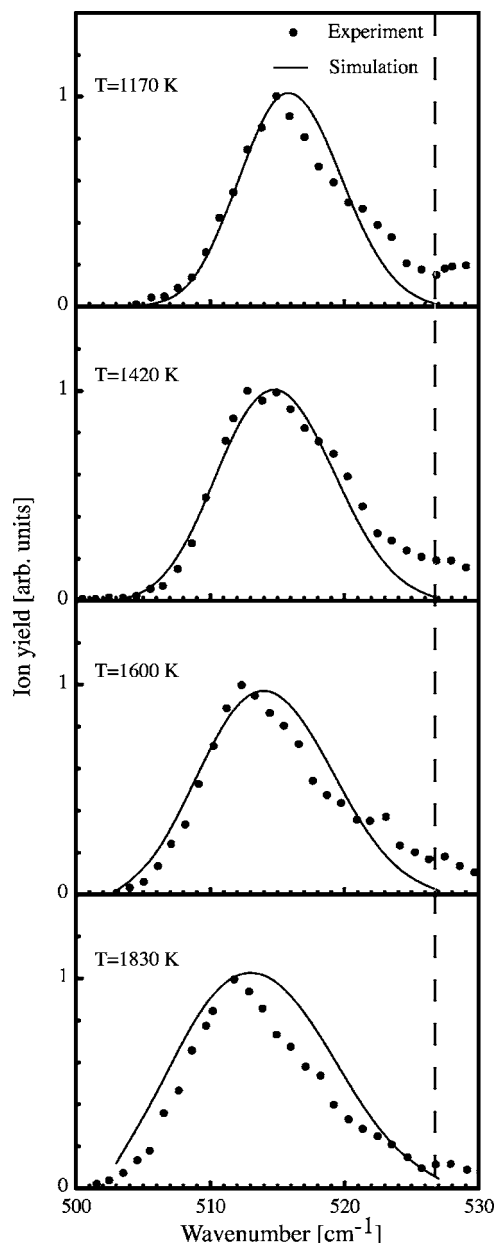


FIG. 8. Experimental (dots) and simulated IR-REMPI spectra around 515 cm^{-1} as a function of temperature. See the text and tables for the parameters employed. Shown as dashed line is the calculated position of the IR mode at 0 K.

$f = 7.5 \text{ cm}$ mirror with the angle between incident and reflected beam being $\Theta = 23^\circ$. The laser pulse shape is taken as a block function in time with the same time-integrated energy as in the experiment. The set of differential equations (10) was solved numerically.

The experimental data together with the best simulations are shown in Figs. 8 and 9. The best fit parameters are shown in Table II. Adjustable parameters are the anharmonicity parameters a and b , the integral absorption cross section for the I_{comb} band, as well as the FELIX fluences around 500 and 1400 cm^{-1} (50 and 40 mJ per macropulse, respectively). It is observed that the parameters are to some extent coupled. For example, increasing ν_0 can be compensated by increasing a or decreasing the absorption cross section can be compensated by increasing the FELIX fluence. For that reason, all ν_0 as well as all absorption cross sections (besides that of the

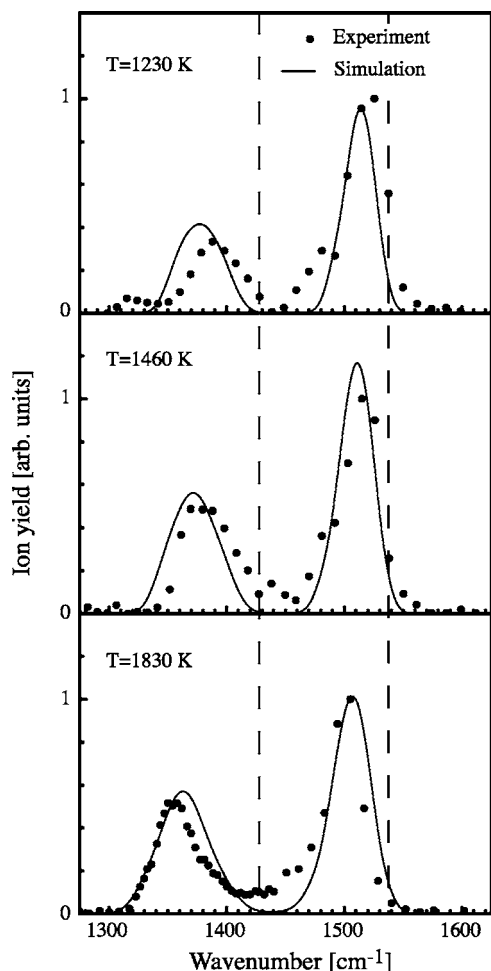


FIG. 9. Experimental (dots) and simulated IR-REMPI spectra in the 1450–1600 cm^{-1} region as a function of temperature. See the text and tables for the parameters employed. Shown as dashed lines are the two calculated positions of the IR active modes at 0 K.

combination band) are held fixed to *ab initio* values. It can be seen that the model reproduces the line positions, shapes, as well as their temperature dependence quite well, giving confidence in the validity of the model employed.

V. DISCUSSION

A surprising observation of the present experiments is that the IR-REMPI spectra of superhot (1790 K) C₆₀ molecules are not very different from that of hot (875 K) C₆₀.¹³ In turn, all IR REMPI spectra, regardless of the temperature of the C₆₀, show close resemblance to the linear (one-photon) IR absorption spectrum of (solid) C₆₀ at room temperature or

TABLE II. The best fit parameters of the IR active vibrational modes and of the combination vibration. ν_0 (cm^{-1}), a ($\text{cm}^{-1}/\text{quant}$), and b ($\text{cm}^{-1}/\text{quant}$) are the spectroscopic parameters of the vibrations used to simulate the shape of the resonances [see (8) and (9)]. The values of A_0 (km/mole) are the integral absorption cross sections defined by the relationships (6).

Type of band	ν_0	a	b	A_0
$F_{1u}(1)$ IR active mode	526.8	0.028	0.008	86.4
$F_{1u}(4)$ IR active mode	1431	0.37	0.075	35.4
I_{comb} combination band	1540	0.2	0.04	7.22

below.²⁶ This is in contrast to what one intuitively might think. One could have expected that, at an internal vibrational energy of almost 20 eV, absorption lines broaden and shift to such an extent that no spectroscopic structure is left over. Instead, well resolved resonances are observed that are separated by regions where no IR-REMPI signal is observed. Especially in the region around 10 μm where powerful CO₂ lasers are available, no signal could be observed, even at the highest temperature. This is significant, as a CO₂ laser has been used in ionization studies of C₆₀ (Ref. 10) and these lasers are frequently used as devices to fragment ions that are stored in ion traps. Their use is then often justified by giving the argument that the IR absorption spectra of internally hot molecules are structureless and all molecules absorb, regardless of their nature.

C₆₀ is with its 174 vibrational degrees of freedom a large molecule. Nonetheless, it is to some extent a special case as it has such a high symmetry and because it is rather rigid with a comparatively high frequency lowest frequency mode at 260 cm^{-1} . One result is that its vibrational modes behave rather harmonically, show only small anharmonic shifts and the low anharmonicities cause only a small amount of broadening. Due to that, the IR excitation process is efficient and the resulting IR-REMPI spectrum is so clean and has such a similarity to the “regular” IR absorption spectrum.

The observed spectrum can be simulated by a simple model. In this model, the absorption process is described by a sequential absorption of single IR photons, every time followed by fast energy redistribution. The anharmonic shift and broadening is assumed to be linear with internal energy. The model describes the observations surprisingly well. Only a few parameters are adjusted and the frequency shifts and peak shapes are reproduced quite well. Nonetheless, the agreement is not perfect. At the highest temperatures, peaks are predicted by the model to be wider than observed. Also, the peak with $\nu_0=1431 \text{ cm}^{-1}$ is observed to shift more with temperature than can be modeled. Obviously, having both ν_0 and the anharmonicity constant a as adjustable parameters can result in a very good fit, but this would, however, yield an unreasonable ν_0 . It might be possible that a linear description of a with internal energy is not sufficient. It is, however, also clear that not enough experimental data are available to address that point and including more adjustable parameters in the model might yield perfect fits, however, also perhaps physically meaningless parameters. A similar situation holds true for the possibility of neutral C₆₀ to fragment instead of ionize. In the model, fragmentation can be included; however, the fit of the model to the experiment is not sensitive to the fragmentation rate constant. We therefore decided to set the fragmentation rate constant arbitrarily to zero and to ignore that point.

One interesting point of IR excitation is that potentially very narrow energy distributions can be obtained. When the absorption of single photons occurs statistically and the absorption probability is only weakly dependent on internal energy, a Poisson distribution of internal energies is created with an average energy of $\bar{n}h\nu$ (\bar{n} =mean number of photons absorbed) and a width of $\sqrt{\bar{n}h\nu}$, i.e., with a relative width $\sim 1/\sqrt{\bar{n}}$. Such a distribution can be wide, when, for ex-

ample, performing UV excitation or, in the case of IR photons, very narrow. In fact, when exciting with photons of about 500 cm^{-1} energy, such a distribution can be narrower than a thermal distribution with the same average energy. In practice, however, the distribution after excitation with photons will look different from a Poisson distribution. One reason for this is that such a distribution needs to be convoluted with the laser spatial profile. When using a focused Gaussian beam one can show that such a distribution is peaked at zero,³⁶ as only very few molecules are within the intense part of the laser beam. At high energies the distribution has a fall off that is given by the molecules that sample the most intense part and is approximately like a Poissonian distribution. Thus, the fall off will be slow when the excitation occurs with UV photons and fast, when the excitation occurs with IR photons. A consequence of the fast fall off is that when exciting with 515 cm^{-1} photons, the hot C_{60} molecules near the high energy cut off of the distribution can either fragment or ionize. However, unless the IR fluence is too high, molecules do not have enough energy to do both. This explains the absence of fragmentation in the mass spectrum after IR excitation at this wavelength and why mass spectra after UV excitation always show extensive fragmentation. When exciting around 1400 cm^{-1} , a large amount of fragmentation is observed, contrary to what is predicted by the above arguments. A reasonable explanation is the sequential absorption of photoproducts during the laser pulse. This can happen, as both C_{60}^+ as well as C_{58} are predicted to absorb strongly at this photon energy while they do not around 520 cm^{-1} . The absorption of those photoproducts can be so strong that fragmentation down to C_{32}^+ can be observed. Unfortunately, we can here give only those qualitative arguments as a more quantitative description would require the knowledge of precise binding and ionization energies.

VI. SUMMARY

The IR-REMPI method, based on the absorption of hundreds of IR photons from a free electron laser, was coupled with a superhot C_{60} beam source. Thermal energy dependent IR-REMPI spectra ($450\text{--}1800\text{ cm}^{-1}$) were measured over the temperature range of $1170\text{--}1830\text{ K}$ corresponding to the thermal energy range of $9\text{--}19\text{ eV}$. Well resolved and background free spectra were obtained. A pronounced temperature dependent redshift of the IR absorption lines was observed and was found to be in good agreement with simulations. Especially strong IR absorption was observed at the high frequency modes (the $1350\text{--}1530\text{ cm}^{-1}$ spectral region) leading to extensive fragmentation down to the smallest stable fullerene ion C_{32}^+ . This finding is in sharp contrast to the very weak fragmentation observed following the IR multiphoton excitation of the lowest frequency mode around $510\text{--}520\text{ cm}^{-1}$.

ACKNOWLEDGMENTS

We gratefully acknowledge the support by the *Stichting voor Fundamenteel Onderzoek der Materie* (FOM) in providing the required beam time on FELIX and highly appreciate the skilful assistance by the FELIX staff. This work was supported in part under the "Access to research infrastructure action of the Improving Human Potential Programme" of the European Community. One of the authors (E. K.) would like to acknowledge grants by the Israel Science Foundation, the James Franck program, as well as from FOM.

- ¹E. E. B. Campbell and F. Rohmund, *Rep. Prog. Phys.* **63**, 1061 (2000).
- ²R. Ehlich, M. Westerburg, and E. E. B. Campbell, *J. Chem. Phys.* **104**, 1900 (1996).
- ³E. E. B. Campbell, T. Raz, and R. D. Levine, *Chem. Phys. Lett.* **253**, 261 (1996).
- ⁴R. D. Beck, J. Rockenberger, P. Weis, and M. M. Kappes, *J. Chem. Phys.* **104**, 3638 (1996).
- ⁵R. D. Beck, C. Warth, K. May, and M. M. Kappes, *Chem. Phys. Lett.* **257**, 557 (1996).
- ⁶R. Volpel, G. Hofman, M. Steidl, M. Stenke, M. Schlapp, R. Trasel, and E. Salzborn, *Phys. Rev. Lett.* **71**, 3439 (1993).
- ⁷H. Hohman, C. Callegari, S. Furrer, D. Grosenick, E. E. B. Campbell, and I. V. Hertel, *Phys. Rev. Lett.* **73**, 1919 (1994).
- ⁸S. C. O'Brien, J. R. Heath, R. F. Curl, and R. E. Smalley, *J. Chem. Phys.* **88**, 220 (1988).
- ⁹D. Wurz and K. Lykke, *Chem. Phys.* **184**, 335 (1994).
- ¹⁰M. Hippler, M. Quack, R. Schwarz, G. Seyfang, S. Matt, and T. Märk, *Chem. Phys. Lett.* **278**, 111 (1997).
- ¹¹E. E. B. Campbell, G. Ulmer, and I. V. Hertel, *Phys. Rev. Lett.* **67**, 1986 (1991).
- ¹²P. Wurz and K. R. Lykke, *J. Chem. Phys.* **95**, 7008 (1991).
- ¹³G. von Helden, I. Holleman, G. M. H. Knippels, A. F. G. van der Meer, and G. Meijer, *Phys. Rev. Lett.* **79**, 5234 (1997).
- ¹⁴G. von Helden, I. Holleman, A. J. A. van Roij, G. M. H. Knippels, A. F. G. van der Meer, and G. Meijer, *Phys. Rev. Lett.* **81**, 1825 (1998).
- ¹⁵G. von Helden, I. Holleman, M. Putter, A. J. A. van Roij, and G. Meijer, *Chem. Phys. Lett.* **299**, 171 (1999).
- ¹⁶D. van Heijnsbergen, G. von Helden, B. Sartakov, and G. Meijer, *Chem. Phys. Lett.* **321**, 508 (2000).
- ¹⁷G. von Helden, I. Holleman, G. Meijer, and B. Sartakov, *Opt. Express* **4**, 46 (1999).
- ¹⁸G. von Helden, D. van Heijnsbergen, and G. Meijer, *J. Phys. Chem. A* **107**, 1671 (2003).
- ¹⁹E. Kolodney, B. Tsipinyuk, and A. Budrevich, *J. Chem. Phys.* **102**, 9263 (1995).
- ²⁰B. Tsipinyuk, A. Budrevich, and E. Kolodney, *J. Phys. Chem.* **100**, 1475 (1996).
- ²¹E. Kolodney, B. Tsipinyuk, and A. Budrevich, *J. Chem. Phys.* **100**, 8542 (1994).
- ²²E. Kolodney, A. Budrevich, and B. Tsipinyuk, *Phys. Rev. Lett.* **74**, 510 (1995).
- ²³A. Bekkerman, B. Tsipinyuk, A. Budrevich, and E. Kolodney, *J. Chem. Phys.* **108**, 5165 (1998).
- ²⁴A. Bekkerman, B. Tsipinyuk, and E. Kolodney, *Int. J. Mass. Spectrom.* **185/186/187**, 773 (1999).
- ²⁵L. Nemes, R. S. Ram, P. F. Bernath, F. A. Tinker, M. C. Zumwalt, L. C. Lamb, and D. R. Huffman, *Chem. Phys. Lett.* **218**, 295 (1994).
- ²⁶K.-A. Wang, A. M. Rao, P. C. Eklund, M. A. Dresselhaus, and G. Dresselhaus, *Phys. Rev. B* **48**, 11375 (1993).
- ²⁷V. Schettino, M. Pagliai, L. Ciabini, and G. Cardini, *J. Phys. Chem. A* **105**, 11192 (2001).
- ²⁸K. Gluch, S. Matt-Leubner, O. Echt, B. Concina, P. Scheier, and T. D. Märk, *J. Chem. Phys.* **121**, 2137 (2004).
- ²⁹R. L. Murry, D. L. Strout, G. K. Odom, and G. E. Scuseria, *Nature (London)* **366**, 665 (1993).

- ³⁰ A. D. Boese and G. E. Scuseria, Chem. Phys. Lett. **294**, 233 (1998).
- ³¹ S. Diaz-Tendero, M. Alcamì, and F. Martin, J. Chem. Phys. **119**, 5545 (2003).
- ³² S. Tomita, J. U. Andersen, K. Hansen, and P. Hvelplund, Chem. Phys. Lett. **382**, 120 (2003).
- ³³ S. Tomita, J. U. Andersen, C. Gottrup, P. Hvelplund, and U. V. Pedersen, Phys. Rev. Lett. **87**, 073401 (2001).
- ³⁴ Assuming a temperature dependent radiative energy loss rate $C(dT/dt) = AT^q(\text{eV s}^{-1})$ along some flight time t , one gets the time dependent temperature $T(T_0, t) = T_0 \left[\frac{(q-1)A/C}{T_0^{q-1}t + 1} \right]^{1/(1-q)}$ with T_0 as the initial (nozzle) temperature and $C = 0.014(\text{eV K}^{-1})$ as the C₆₀ heat capacity (Ref. 19). Using $A = 4.5 \times 10^{-17} \text{ eV s}^{-1} \text{ K}^{-6}$ and $q = 6$ (Ref. 33) we get an average energy loss of 0.95 eV for $T_0 = 1830 \text{ K}$ and 0.48 eV for $T_0 = 1600 \text{ K}$ ($t = 0.66 \text{ ms}$).
- ³⁵ E. Kolodney, B. Tsipinyuk, and A. Bekkerman, Fullerene Sci. Technol. **6**, 67 (1998).
- ³⁶ K. Mehlig, K. Hansen, M. Hedén, A. Lassesson, A. V. Bulgakov, and E. E. B. Campbell, J. Chem. Phys. **120**, 4281 (2004).